One-step phenol production from a water–toluene mixture using radio frequency in-liquid plasma

Muhammad AGUNG[1,2]**, Shinfuku NOMURA**[1,4]**, Shinobu MUKASA**[1]**, Hiromichi TOYOTA**[1]**, Otsuka KAZUHIKO**[1] **and Hidekazu GOTO**[3]

[1] Graduate School of Science and Engineering, Ehime University, Matsuyama 790-8577, Japan
[2] Faculty of Engineering, Makassar State University, Makassar 90-222, Indonesia
[3] Graduate School of Engineering, Osaka University, Suita 565-0871, Japan

E-mail: nomura.shinfuku.mg@ehime-u.ac.jp

CrossMark

Abstract

The objectives of this research were to understand the process of converting toluene into phenol in a one-step process directly from a water–toluene mixture using the plasma in-liquid method. Experiments were conducted using 27.12 MHz radio frequency (RF) in-liquid plasma to decompose a solution of 30% toluene. Based on the experimental results as evaluated using gas chromatography–mass spectrometry (GC–MS), along with additional analysis by the Gaussian calculation, density functional theory (DFT) hybrid exchange–correlational functional (B3LYP) and 6-311G basis, the phenol generated from toluene was quantified including any by-products. In the experiment, it was found that OH radicals from water molecules produced using RF in-liquid plasma play a significant role in the chemical reaction with toluene. The experimental results suggest that phenol can be directly produced from a water–toluene mixture. The maximum phenol yields were 0.0013% and 0.0038% for irradiation times of 30 s and 60 s, respectively, at 120 W.

Keywords: phenol, toluene, radio frequency, in-liquid plasma, Gaussian calculation

(Some figures may appear in colour only in the online journal)

1. Introduction

Phenol is one of the compounds used as a raw material for resins and other widely used chemicals [1, 2]. World production exceeded 11 million tons in 2009 [3]. Presently, most phenol is produced industrially through the cumene process [1, 2, 4–7] and toluene oxidation [2, 4, 5, 7], which accounts for more than 90% of the world phenol production. The cumene process consists of three reactions; alkylation of benzene by propylene, oxidation of cumene to cumene hydroperoxide, and decomposition of cumene hydroperoxide to phenol and acetone. The toluene oxidation process consists of two reactions [8]; oxidation of toluene and oxidative decomposition of benzoic acid [9].

The cumene process has the main advantage of using two relatively inexpensive starting materials, benzene and propylene, which are subsequently converted into two more useful products, phenol and acetone. In spite of these positive aspects, the cumene process has some disadvantages such as a high environmental impact [3, 5], an explosive intermediary compound (cumene hydroperoxide) [5, 10], use of a corrosive catalyst [5], production of unwanted impurities [5, 7]. It is a multi-step process, which makes it hard to obtain high phenol yields with respect to the amount of benzene used and requires high energy consumption due to its characteristic multi-step process [11]. On the other hand, the toluene oxidation process requires only two steps, but the phenol production result is very low compared to the cumene process [4, 8, 9]. Therefore, a process whereby phenol can be formed

[4] Author to whom any correspondence should be addressed.

in a one-step process with high yield and selectivity is highly desired.

Many researchers have reported the use of benzene in a one-step process in a variety of methods. Use of a variety of catalysts for the direct hydroxylation of benzene to phenol [7, 12], photochemical systems [11, 13], and electrochemical oxidation systems [11] have been extensively investigated.

Unlike studies on making phenol in one-step using benzene, there have been few, if any, studies examining the manufacture of phenol using toluene in a single-step process. Therefore, the results of this research should provide some new insights into the one-step phenol production method. Toluene is less toxic and more reactive than benzene and is normally cheaper [8]. Moreover, benzene is commonly produced from toluene. These two facts alone illustrate the significant advantage of creating phenol with a water–toluene mixture using a single-step RF plasma in-liquid method. The idea of mixing toluene with pure water to form phenol is based on the simple assumption that by using the RF plasma in-liquid method, the toluene will produce various benzene derivatives and the pure water will generate the free radicals needed for the hydroxylation and oxidation process to convert the benzene derivatives to phenol.

The in-liquid plasma method is used to generate high-frequency plasma inside bubbles in a liquid by microwaves (MW) [14] or RF [15]. The electron temperature as measured from the emission intensity ratio of H_α and H_β is calculated to be from 3000 K to 5000 K [16]. The high temperature and atmospheric pressure platform inside the plasma bubbles can also complement the reaction process. The application of RF in-liquid plasma has been proven to produce molecular oxygen and hydrogen, oxygen, hydroxyl, hydroperoxyl, hydrogen peroxide, and other reactive radicals [15, 17] and is key to direct hydroxylation and oxidation of a toluene solution. Additionally, the RF in-liquid plasma method can be used to decompose methane hydrate [18, 19], methylene blue [20], glucose and cellulose [21, 22] and other such organic liquids [23]. For the present study, the possibility of single step production of phenol from a toluene–water mixture using RF in-liquid plasma was investigated.

2. Experimental method and analysis

The experimental apparatus is shown schematically in figure 1. A copper brass container (56 mm outside diameter (OD), 21 mm inside diameter (ID)) was used as the vessel. Two inspection windows of transparent quartz glass were provided in the front and rear of the vessel with a spectroscopy probe positioned just outside the front window, directed into the vessel. An electrode composed of a copper rod with a diameter of 3 mm inserted into a transparent quartz tube (6 mm OD) was provided from the bottom of the vessel. A counter electrode composed of a brass pipe 75 mm long with an outer diameter of 6 mm and an inner diameter of 4 mm was inserted from the top of the vessel. The distance between the electrode and counter electrode was 1.5 mm. The head of the electrode was shaped to be hemispherical to promote easy plasma
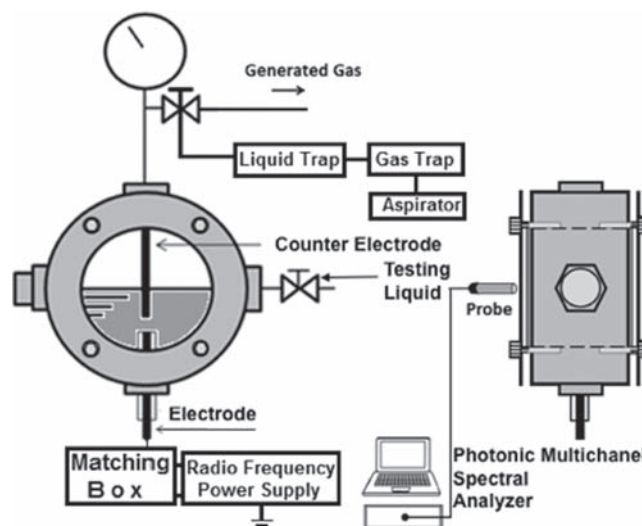

Figure 1. Experimental apparatus.

generation. The pressure throughout the system was reduced using an aspirator and maintained between 0.01–0.02 MPa.

Pure water is water that has been demineralized and has the following properties: a temperature of 25 °C, conductivity of 2 μS cm^{-1}, and pH of 6.54. A water–toluene mixture is a solution composed of pure water and toluene. In this study, the 10 ml of water–toluene solution used had the following initial conditions: a concentration of 30%, temperature of 25 °C, conductivity of 3.6 μS cm^{-1}, and pH of 6.65. This solution was injected by a syringe into the vessel, which had a maximum volume capacity of 15 ml. No additional solution was needed during the experiment. The vessel was 2/3 filled with the water–toluene solution, with the remaining 1/3 filled with air. To generate RF in-liquid plasma, a matching box and 27.12 MHz RF generator were used together to control input power and impedance. The input power was varied at 100 W, 110 W, 120 W, and 130 W and combined with plasma irradiation times of 30 s and 60 s. The power values were calculated by subtracting the reflected power from the forward power.

2.1. Spectroscopic analysis

Two spectroscopic analyses were conducted. The first analysis was conducted by a multichannel spectral analyzer (Hamamatsu Phototonics PMA-11 C7473-36), which was used to identify the product from the toluene solution during plasma generation in the liquid solution. The exposure time for the spectrum measurement was 50 ms and the spectrum values from five emissions were used to determine the average values and standards of deviation. For the second analyses, the liquid samples generated by RF in-liquid plasma were analyzed using a GC–MS Thermo Scientific TQ 900. These analyses were conducted to measure the chemical product of toluene decomposition.

GC–MS was conducted with a helium carrier gas, split injection mode, 1 μl injection volume, 200 °C inlet temperature, 45 kPa pressure, 30 m length $\times$ 0.25 μm thickness $\times$ 0.25 mm ID capillary column, and temperature programming of 40 °C
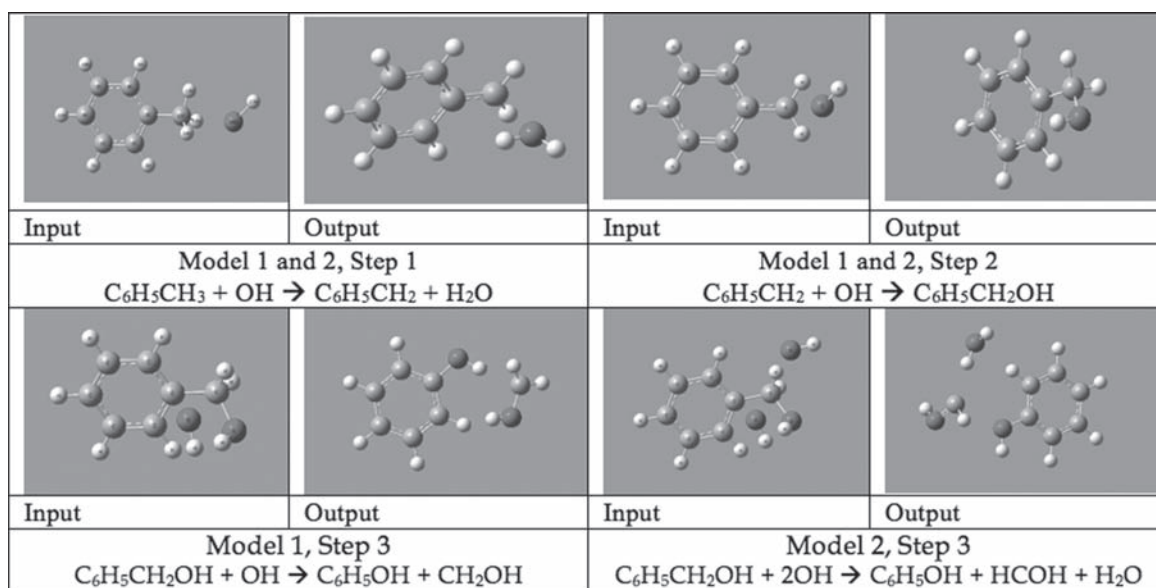
Input	Output
Model 1 and 2, Step 1 $C_6H_5CH_3 + OH \rightarrow C_6H_5CH_2 + H_2O$	

Input	Output
Model 1 and 2, Step 2 $C_6H_5CH_2 + OH \rightarrow C_6H_5CH_2OH$	

Input	Output
Model 1, Step 3 $C_6H_5CH_2OH + OH \rightarrow C_6H_5OH + CH_2OH$	

Input	Output
Model 2, Step 3 $C_6H_5CH_2OH + 2OH \rightarrow C_6H_5OH + HCOH + H_2O$	

Figure 2. Mechanism reaction of toluene with OH radicals to produce phenol using Gaussian calculation models 1 and 2.

(maintained for 5 min), 250 °C (maintained for 5 min) and 40 °C. When employing the GC–MS method, a slightly yellowish colored liquid remained in the vessel after each experimental RF in-liquid plasma cycle. The liquid is composed of two phases, a chemical mixture phase on top and a water phase below. A 10 μl liquid sample was taken from the chemical mixture phase and put into a bottle. Then, 1000 μl of methanol was added to the bottle to mix with the 10 μl liquid sample. A 1 μl liquid sample was then taken from the mixture bottle and injected to the GC–MS for quantitative analysis. In the next step, pure standard samples (Toluene, Wako 203-18465, 99.5%; Benzene, Wako 025-06691, 99.7%; Benzyl Alcohol, Wako 027-01276, 99.0%; Formaldehyde, Wako 063-04815; O-Cresol, Wako 036-16372, 99%; and M-Cresol, Wako 036-20922, 99%) were used to plot individual calibrations. Subsequently, the prevailing concentration of the experimental product was revealed by comparing the experimental peak area with those obtained by calibration of the standards at the respective retention times. The standard listing of NIST was used to examine and compare with the mass spectrometric (MS) fragmentation patterns at matching peak retention times. The error of the GC–MS analyses remained within ±5%.

2.2. Gaussian calculation analysis

The purpose of the calculations was to investigate the reaction route of toluene to phenol by OH radicals with no potential barrier. It was assumed that toluene decomposition and phenol production reactions are induced from attacks by OH radicals produced by plasma in water. It is also assumed that the OH radicals are constantly and sufficiently supplied to the toluene molecule.

Under the above assumptions, configuration optimization [24] was undertaken using Gaussian calculations under the condition that there are only one toluene molecule and one OH molecule located near the methyl group (–CH$_3$).
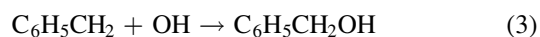
Geometry optimization usually attempts to locate the minima on the potential energy surface. Optimization can be used to locate transition structures. All optimization calculations were done within the framework of DFT B3LYP with 6-311G basis [25] using the Gaussian 09W program [26]. By applying this framework, the theoretical reaction mechanism of water–toluene mixed decomposition can be predicted for known products and byproducts. Moreover, the Gaussian calculation analysis is adequate for the prediction of a significant number of properties of molecules and reactions, comprising the following: sub-atomic energies and structure, sub-atomic orbitals, energies and structures of transition states, bond and result energies, multipole moments, atomic charges and electrostatic possibilities, infrared (IR) and Raman spectra, vibrational frequencies, nuclear magnetic resonance (NMR) characteristic, thermochemical characteristic, polarizabilities and hyperpolarizabilities, and reaction pathways [24]. However, the Gaussian calculations in this research are only limited to predicting the reaction pathways.

Two models of the complete reaction of toluene with OH radicals were proposed for producing phenols based on the Gaussian calculation. The difference between model 1 and model 2 is only at step 3 (equations (4) and (8)) for each model as shown in figure 2. In another calculation, different models for step 3 were attempted by including 3OH and 4OH radicals. However, phenol is not formed. The following step shows the mechanism reaction of phenol.

- Model 1

$$C_6H_5CH_3 + 3OH \rightarrow C_6H_5OH + CH_2OH + H_2O \quad (1)$$

The detailed process of model 1 is as follows

$$C_6H_5CH_3 + OH \rightarrow C_6H_5CH_2 + H_2O \quad (2)$$

$$C_6H_5CH_2 + OH \rightarrow C_6H_5CH_2OH \quad (3)$$

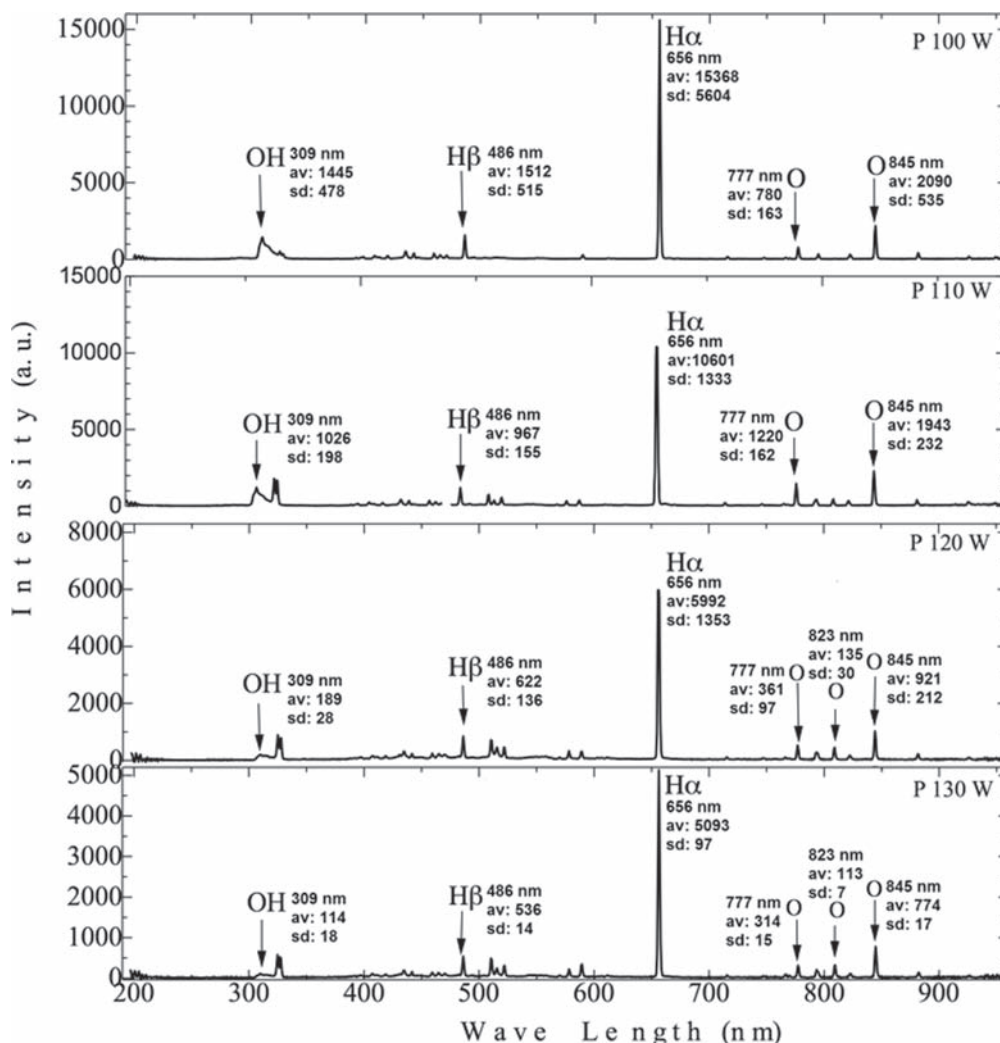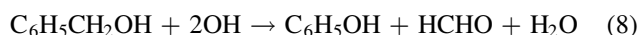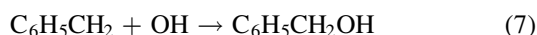**Figure 3.** Emission RF spectrum for a 30% water–toluene mixture at less than atmospheric pressure as a function of power input (100–130 W).

$$C_6H_5CH_2OH + OH \rightarrow C_6H_5OH + CH_2OH \quad (4)$$

- Model 2

$$C_6H_5CH_3 + 4OH \rightarrow C_6H_5OH + HCHO + 2H_2O \quad (5)$$

The detailed process of model 2 is as follows

$$C_6H_5CH_3 + OH \rightarrow C_6H_5CH_2 + H_2O \quad (6)$$

$$C_6H_5CH_2 + OH \rightarrow C_6H_5CH_2OH \quad (7)$$

$$C_6H_5CH_2OH + 2OH \rightarrow C_6H_5OH + HCHO + H_2O \quad (8)$$

3. Results and discussion

3.1. Plasma emission spectrum

RF power was irradiated from the electrode, with the electrode heating and simultaneously generating water-vapor

bubbles. Plasma was then immediately ignited inside the bubbles, and a bright sphere appeared at the head of the 3 mm diameter copper electrode with the plasma region touching the counter electrode. Plasma generated from this in-liquid plasma was non-thermal plasma. One of the characteristics of non-thermal plasma is that the electron temperature is much higher than that of vapor gas (in the macroscopic temperature plasma region inside the bubble). The temperature of this boundary condition was low near the ambient temperature of the surrounding liquid and the plasma was formed at near atmospheric pressure. This type of plasma is clearly not filamentary or uniform plasma. It was clearly observed that the plasma emission was continuous. The color of the regional plasma was violet and at the top, the local plasma was bright white. The diameters of the plasma and surrounding bubble were approximately 3 mm and 6 mm, respectively.

Figure 3 shows the typical optical emission spectrum of a toluene solution by RF in-liquid plasma. Using the multi-channel spectral analyzers during plasma formation with
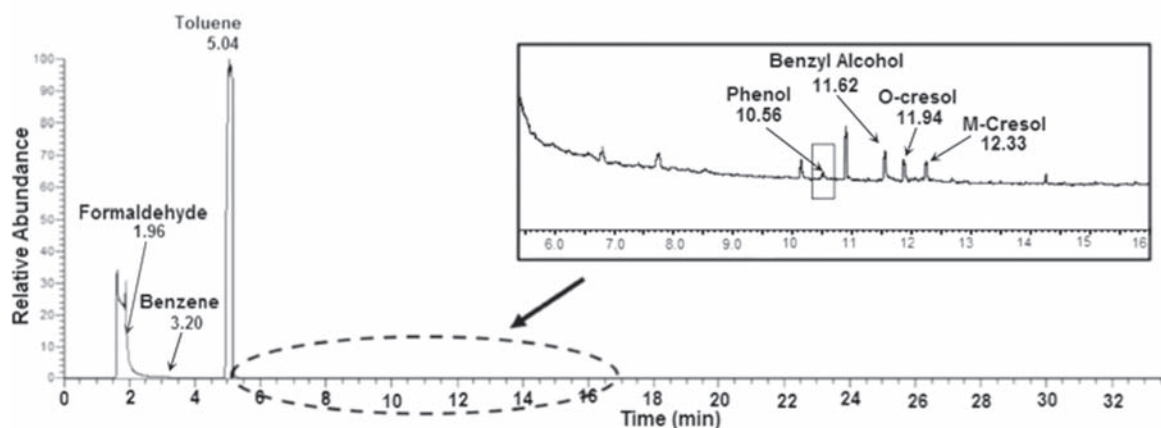
4

Figure 4. Typical graph pattern of the experimental results for toluene decomposition by RF in-liquid plasma as analyzed by GC–MS (120 W with 60 s irradiation sample).

power 100 W to 130 W, the emission spectra of the species of OH (309 nm), H_β (486 nm), H_α (656.3 nm) and O (777 nm and 845 nm) were observed. The results of the emission spectra in this study were similar to those in the study of Wang *et al* [27] for which microwaves were used. The emission spectrum of the OH species at 309 nm was the excited-state for OH radicals [28] and the other emission spectrum species were excited reactive atoms [29]. At 120 W and 130 W, a new emission spectrum of the species O emerged at 823 nm. This condition suggests that increasing the discharge power will increase the number of excited reactive atom species of O. However, the emission intensity for all species will decrease due to the increased discharge power. The increased heat from the electrode is caused by the increased discharge power, which creates more bubbles that obscure the intensity of the emissions in the solution surrounding the plasma. Under this condition, the intensity of the emission captured by the probe will decrease.

All of the above excited reactive species are the products of water decomposition during plasma ignited in the toluene solution. The major reactions for the production of reactive species for the formation of ground state OH and H in-liquid plasma are as follows: (1) e + H_2O → OH + H + e (2) e + H_2O → OH + H^- and (3) e + H_2O^+ → OH + H with reaction rate ($m^3 s^{-1}$) 2.3×10^{-18} to 1.8×10^{-16}, 4.9×10^{-18} to 4.7×10^{-17}, and 2.6×10^{-14}, respectively [29].

The formation process of the excited reactive and radicals in this study was as follows. The process begins when the water bubbled at the interface side. At this time, the evaporated water molecules were initially decomposed to H and O excited reactive atoms along with the generation of OH radicals. The OH radicals are formed from the liquid-phase water when the solution is exposed to the plasma. The OH radicals in the excitation state that caused the emission were generated by direct excitation from the ground state or dissociated recombination of water cations (H_2O^+) [30]. A sufficient amount of water cations was assumed because the

ionization energy of water is relatively low, and effectively dissociated recombination occurred by thermal electrons that were far from the electrode. It is believed that OH radicals directly react with liquid-phase toluene molecules at the gas–liquid interface in a number of pathways. With these direct reactions, OH radicals perform an important function in the decomposition of a toluene solution into many chemical substances.

3.2. Laboratory findings

Primary product identification. In the output from the liquid residue sample, seven major products are found: toluene ($C_6H_5CH_3$), phenol (C_6H_5OH), benzene (C_6H_6), benzyl alcohol ($C_6H_5CH_2OH$), formaldehyde (HCHO), O-cresol and M-cresol (C_7H_8O), which were identified based on the GC–MS spectra collected, as shown in figure 4.

Regarding the Gaussian calculation in model 2, identical results were found in the experimental products. This model seems appropriate due to the observation of benzyl alcohol ($C_6H_5CH_2OH$) and formaldehyde (HCHO). The reaction mechanism of toluene +OH radicals as shown in equations (2) and (6) has been previously reported (e.g. Huang *et al* [31] and Seta *et al* [32]). Benzyl radicals as a product will react with other OH radicals forming benzyl alcohol as shown in equation (7). Then benzyl alcohol with 2OH radicals forms phenol, formaldehyde, and water as shown in equation (8).

The phenol yield (%) is a ratio of the quantity of produced phenol from the detected phenolic quantity (Ph = mol) divided by the quantity of initial toluene (T_i = mol) in the concentrated water–toluene mixture solution. The calculation formula for the phenol yield is shown in equation (9)

$$\text{phenol yield (\%)} = \frac{Ph}{T_i} \times 100. \qquad (9)$$
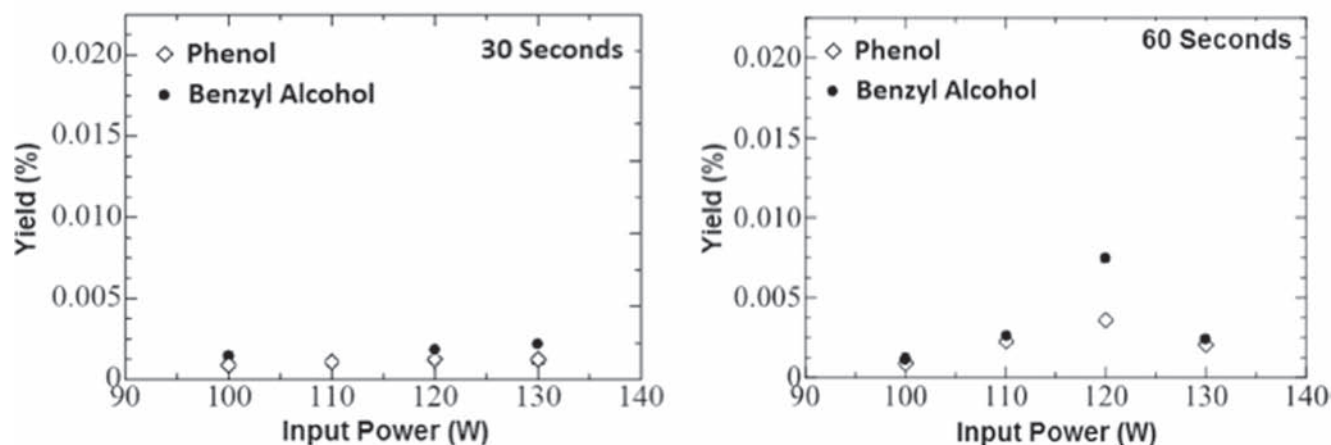
Figure 5. Benzyl alcohol and phenol yield from the decomposition of water–toluene by RF in-liquid plasma: (a) plasma irradiation of 30 s and (b) plasma irradiation of 60 s.

Similarly, the yield calculation formula can be applied to benzyl alcohol, formaldehyde, benzene, O-cresol and M-cresol, based on the detected quantity of each product in the resulting experiment.
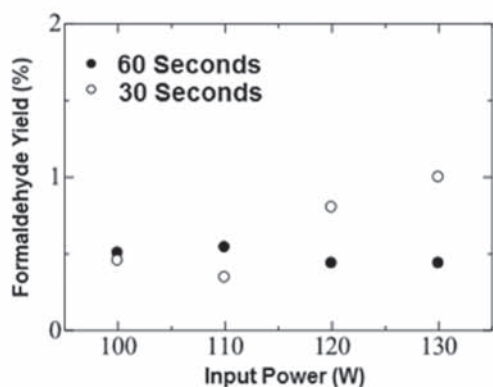
Figure 5 shows the trend of the graph of the benzyl alcohol yield, which can be seen when the graphs are compared. This trend is in line with the reaction predicted by Gaussian calculation of the steps of the process for producing phenol. From here, it can be seen that one stage early in the process of toluene decomposition produced benzyl alcohol, which eventually formed phenol. In other words, during phenol generation, benzyl alcohol is more likely to be formed as an intermediate product.

All the analysis results from the 30 s and 60 s experiments show (figures 5(a) and (b)) that phenol production by 60 s irradiation is higher than that by 30 s irradiation. This is thought to be because the extra plasma radiation time may yield a chain reaction producing more phenol. The maximum phenol yields in this experiment were 0.0013% and 0.0038%, for irradiation times of 30 and 60 s respectively at 120 W as shown in figures 5(a) and (b). Despite the resulting small production of phenol, several advantages may be considered related to energy efficiency. The first advantage is that this process step is only a single step compared to the 3-step cumune process or the conventional 2-step process [8] for converting toluene to phenol. The second advantage is that this approach does not require any catalysts. Another benefit of this research is the successful conversion toluene to phenol at low pressure (less than atmospheric pressure). Thus, when these three advantages are taken into consideration, it can be ascertained that this method is better from an energy efficiency standpoint. Further research is expected to increase the phenol yield. However, there have been no studies examining the manufacture of phenol using toluene in a single-step process. The novelty of this study is the success of producing phenol with a single step process using RF in-liquid plasma.
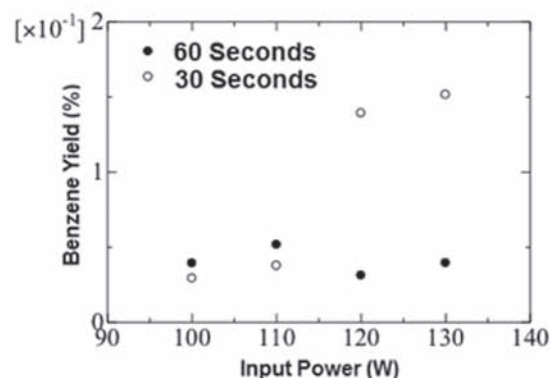
Besides the formation of an intermediate product that leads to the formation of the phenol product, another reason for the low production of phenol is the amount of byproducts during the decomposition process of toluene as shown in figures 6(a)–(d). In figures 6(a)–(d), byproducts of toluene, namely formaldehyde, benzene, O and M-Cresol at 30 s and 60 s, can be seen. Every byproduct in figures 6(a)–(d) has a greater value than the phenol formed from the decomposition of toluene.

Based on the Gaussian calculation, O-cresol is formed by the reaction of toluene and 2OH. Unlike the process for formation of phenol, where an OH radical attacks near the methyl group, the process for creation of O-cresol occurs if the OH radical attacks one of the C–H atoms in the benzene chain. For O-cresol, OH radicals attack the C–H atoms located near the C–CH_3 atoms (right) so that the H atom breaks apart from the C–H bond and the OH radicals formed H_2O molecules. Furthermore, the C atom that has been released from the H atoms by OH radicals attacks other atoms thus forming O-cresol. Under the same mechanism, M-cresol is created through attacks on the C–H bond in toluene, which is far away from the C–CH_3. The reaction of the process of formation of O-cresol using the Gaussian calculation can be seen in figure 7. In order to form benzene, an alternative way to decompose toluene is possible, which is triggered by the radical species H_β, H_α, and O attacking methyl groups (–CH_3). The separated methyl group causes the molecule to become a phenyl radical (C_6H_5) with H_β and H_α merging into benzene. From the comparison of figures 6(b) and (a), it can be seen that the benzene yield is smaller than that of formaldehyde. This means that the formation of benzene from toluene was a multistep process such as the manner in which formaldehyde is formed.
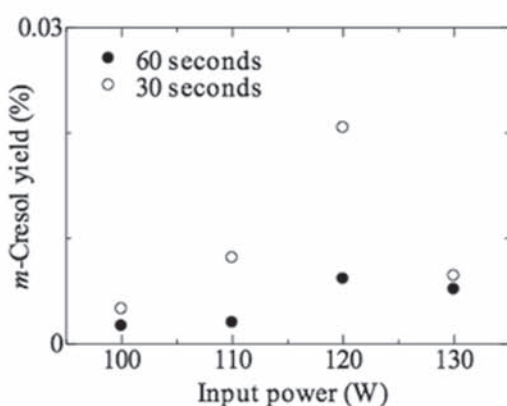
In future research, a higher concentration of the water–toluene mixture with variations in pressure, power, and irradiation time will be investigated with the aim of increasing the phenol yield.
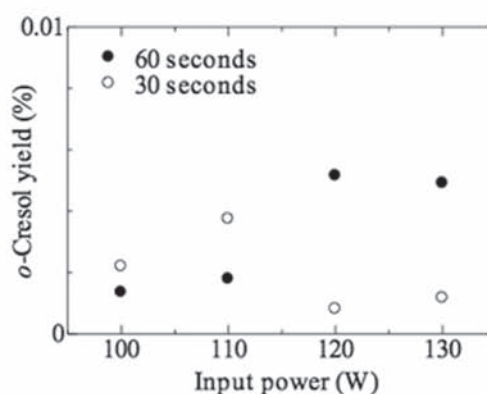
Figure 6. (a) Formaldehyde yield (b) benzene yield (c) M-cresol yield and (d) O-cresol yield as byproducts of the decomposition of a water–toluene mixture using RF in-liquid plasma.
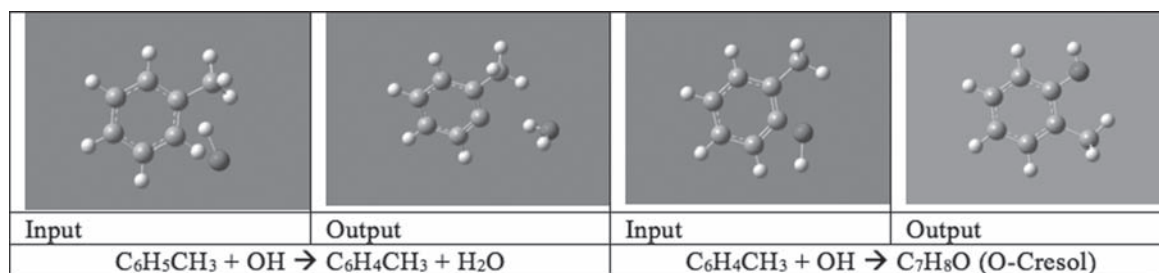

Input	Output	Input	Output
$C_6H_5CH_3 + OH \rightarrow C_6H_4CH_3 + H_2O$		$C_6H_4CH_3 + OH \rightarrow C_7H_8O$ (O-Cresol)	

Figure 7. Mechanism of O-cresol formation from toluene and OH radicals.

4. Conclusions

The initial findings of this study provide a clear understanding of the mechanism of the phenol generation process, and comes to the conclusion that the RF in-liquid plasma method becomes more attractive. Species radicals of OH (309 nm), H_β (486 nm), H_α (656.3 nm) and O (777 nm, 823 nm and 845 nm) were generated by inducing the water molecule using RF in-liquid plasma in the range power of 100 W to 130 W. These radical species that decompose molecules of toluene to

form phenol and other products were identified clearly from the results of GC–MS analysis.

The RF in-liquid plasma at 27.12 MHz was carried out to confirm that one-step phenol production from 30% toluene solution is possible. The mechanism of the formation process of phenol from toluene begins with the formation of OH radicals from water molecules, which then attack toluene molecules at the location near the methyl group (–CH$_3$) to form the benzyl radical (C$_6$H$_5$CH$_2$). Afterward, the benzyl radicals at the location methanedhyl (–CH$_2$) will attract one

other OH radical to form benzyl alcohol (C$_6$H$_5$CH$_2$OH). Finally, the benzyl alcohol reacts with one or two OH radicals to form phenol. The maximum phenol yields were 0.0013% and 0.0038% for irradiation times of 30 s and 60 s respectively at 120 W. The laboratory findings in which phenol and byproducts were produced can be explained and supported by Gaussian calculations. The Gaussian calculations were conducted within the framework of DFT B3LYP and on a 6-311G basis.

Acknowledgments

References

[1] Rappoport Z 2003 *The Chemistry of Phenols 1* (Hoboken, NJ: Wiley-Interscience) pp 3–20
[2] Tyman J H P 1996 *Synthetic and Natural Phenols* (Netherlands: Elsevier) p 22
[3] Zakoshansky V 2009 *Russian J. Gen. Chem.* **79** 2267
[4] Miyake T *et al* 2002 *J. Molec. Catal. A: Chem.* **178** 199
[5] Horváth B *et al* 2014 *App. Catal. A: Gen.* **481** 71
[6] Sayyar M H and Wakeman R J 2008 *Chem. Engin. Res. Des.* **86** 517
[7] Choi J S *et al* 2004 *J. Ind. Eng. Chem.* **10** 445
[8] Kaeding W W *et al* 1965 *I & E C Process Des. Develop.* **4** 97
[9] Lee B *et al* 2012 *Angew. Chem. Int. Edn* **51** 6961
[10] Molinari R and Poerio T 2009 *Asia-Pacific J. Chem. Engin.* **5** 191
[11] Shoji O *et al* 2013 *Angew. Chem. Int. Edn* **52** 6606
[12] Zhai P *et al* 2005 *Chem. Eng. J.* **111** 1
[13] Molinari R *et al* 2009 *Catal. Today* **144** 81
[14] Nomura S *et al* 2006 *Appl. Phys. Lett.* **88** 114
[15] Maehara T *et al* 2006 *Japan. J. Appl. Phys.* **45** 8864
[16] Mukasa S *et al* 2009 *J. Appl. Phys.* **106** 1
[17] Mukasa S *et al* 2011 *Plasma Sources Sci. Technol.* **20** 034020
[18] Rahim I *et al* 2015 *Appl. Therm. Eng.* **90** 120
[19] Putra A E E *et al* 2012 *Int. J. Hydrog. Energy* **37** 16000
[20] Maehara T *et al* 2008 *Plasma Chem. Plasma Process.* **28** 467
[21] Syahrial F *et al* 2014 *J. Japan Inst. Energy* **1** 1207
[22] Syahrial F *et al* 2015 *Int. J. Hydrog. Energy* **1** 11399
[23] Rahim I *et al* 2015 *J. Power Energy Engin.* **03** 28
[24] Foresman J B and Frisch A 1996 *Exploring Chemistry With Electronic Structure Methods* (Pittsburgh, PA: Gaussian, Inc.) pp 35–9
[25] Lewars E 2003 *Computational Chemistry: Introduction to the Theory and Applications of Molecular and Quantum Mechanics* (New York: Kluwer) p 385-58
[26] Frisch M J *et al* 2015 Gaussian 09 (http://gaussian.com/g_tech/g_ur/m_citation.htm)
[27] Wang B *et al* 2016 *Int. J. Hydrog. Energy* **41** 7280
[28] Kanazawa S *et al* 2011 *Plasma Sources Sci. Technol.* **20** 034010
[29] Yang Y, Cho Y I and Fridman A 2012 *Plasma Discharge in Liquid, Water Treatment and Applications* (Boca Raton, FL: CRC Press) p 22
[30] Bruggeman P and Leys C 2009 *J. Phys. D: Appl. Phys.* **42** 053001
[31] Huang M *et al* 2008 *J. Mol. Struct.: Theochem.* **862** 28
[32] Seta T *et al* 2006 *J. Phys. Chem.* A **110** 5081